Detection of the Mild Emphysema by Quantification of Lung Respiratory Airways With Hyperpolarized Xenon Diffusion MRI

Weiwei Ruan, BS,[1] Jianping Zhong, BS,[1] Ke Wang, BS,[2] Guangyao Wu, MD,[2] Yeqing Han, MS,[1] Xianping Sun, BS,[1] Chaohui Ye, BS,[1] and Xin Zhou, PhD[1]*

Purpose: To demonstrate the feasibility to quantify the lung respiratory airway in vivo with hyperpolarized xenon diffusion magnetic resonance imaging (MRI), which is able to detect mild emphysema in the rat model.

Materials and Methods: The lung respiratory airways were quantified in vivo using hyperpolarized xenon diffusion MRI (7T) with eight b values (5, 10, 15, 20, 25, 30, 35, 40 s/cm^2) in five control rats and five mild emphysematous rats, which were induced by elastase. The morphological results from histology were acquired and used for comparison.

Results: The parameters D_L (longitudinal diffusion coefficient), r (internal radius), h (alveolar sleeve depth), Lm (mean linear intercept), and S/V (surface area to lung volume ratio) derived from the hyperpolarized xenon diffusion MRI in the emphysematous group showed significant differences from those in the control group ($P < 0.05$). Additionally, these parameters correlated well with the Lm obtained by the traditional histological sections (Pearson's correlation coefficients >0.8).

Conclusion: The lung respiratory airways can be quantified by hyperpolarized xenon diffusion MRI, showing the potential for mild emphysema diagnosis. Also, the study suggested that the hyperpolarized xenon D_L is more sensitive than D_T (transverse diffusion coefficient) to detect mild emphysema.

Level of Evidence: 1

Emphysema is a pulmonary disease characterized by the destruction of the lung respiratory airways including respiratory bronchiole, alveolar duct, alveolar sacs, and alveoli, resulting in the enlargement of pulmonary airspaces without fibrosis.[1] It is one of the main features of chronic obstructive pulmonary disease (COPD). Currently, there are 64 million people diagnosed with COPD in the world, and 3 million people die from COPD every year, which is predicted to become the third leading cause of death worldwide by 2030 according to World Health Organization (http://www.who.int/respiratory/copd/en/). Pulmonary function tests (PFTs) and high-resolution computed tomography (CT) are common methods used to diagnose emphysema. Patients with emphysema have a decreased expiratory flow rate, but as much as 30% of lung capacity can be lost before changes appear in PFTs.[2] Thus, PFTs are insensitive to the initial stages of emphysema. CT has substantially greater value for evaluation of emphysema, because the enlargement of airspaces will reduce X-ray attenuation and exhibit a lower attenuation on the image, but other factors may also reduce the attenuation, such as a decreased perfusion or air trapping.[3] More important, the use of CT in longitudinal studies is limited because of ionizing radiation exposure.

Magnetic resonance imaging (MRI) does not use ionizing radiation and therefore can be used repeatedly in longitudinal studies. However, MRI of the lung airways is impossible due to the exceedingly low density of nuclear spins present in the airspace. Hyperpolarized (HP) gas (^{3}He or ^{129}Xe) MRI is an emerging modality for quantifying anatomical and functional characteristics of lungs in vivo.[4] With the laser-based spin exchange or metastability-exchange process, the nuclear spins of ^{3}He or ^{129}Xe atoms

can achieve a high nonequilibrium nuclear spin polarization that provides a strong MR signal, making lung MRI possible.[5] In addition, the sublimation DNP (dynamic nuclear polarization) has also demonstrated feasibility to hyperpolarize ^{129}Xe at a polarization level and in quantities that are sufficiently large for biomedical applications.[6] Hyperpolarized gas diffusion MRI of lungs has shown a remarkable sensitivity to pulmonary diseases,[7,8] especially emphysema.[9,10] The apparent diffusion coefficient (ADC) of hyperpolarized gas in the emphysematous lungs will increase due to the pulmonary tissue expansion and alveolar destruction.[11,12]

Previous studies of HP gas diffusion MRI have focused on ^{3}He. Unfortunately, the rarity of ^{3}He on Earth and its rapidly increasing cost have severely limited the broader use of HP ^{3}He MRI. These limitations have led to a transition to less expensive and more available nuclei such as ^{129}Xe.

Mugler et al. first demonstrated measurements of ^{129}Xe ADCs in healthy human volunteers.[13] Mata et al. demonstrated that ^{129}Xe ADCs for rabbits in an emphysematous group increased significantly compared to those of a control group when the b parameter was 10 s/cm.[14] However, the diffusion of hyperpolarized gas in the lung was non-Gaussian, which was manifested through nonexponential signal decay when images were acquired using large b-values.[15] It would be more reasonable to describe the diffusion by fitting signal decays with increased b values.[15] Moreover, it became possible to acquire pulmonary morphological parameters in vivo with multi-b diffusion MRI. Yablonskiy et al. established quantitative relationships between lung morphology and HP gas diffusion MRI by theoretical analysis and computer simulations[16,17] according to the lung simplified model as shown in Fig. 1.[10] They first measured lung geometrical parameters in vivo at the acinar level with ^{3}He diffusion MRI and demonstrated substantial differences between healthy and emphysematous lungs.[18] They then used the same method to evaluate emphysematous disease progression in canine models, and also showed that this method could provide important regional information on lung microstructure, potentially improving the evaluation of emphysematous progression.[19] In the latter theoretical analysis[16,17] and experiments,[20,21] they also took into account the effects of the dependence of longitudinal diffusion coefficient (D_L) and transverse diffusion coefficient (D_T) on b-value. Recently, the method was also used to provide direct experimental evidence for age-related adaptive changes in human acinar airways.[22]

The measurement of gas diffusion properties from multi-b values requires a high image signal-to-noise ratio (SNR) for good accuracy in fitting of lung geometric parameters.[23,24] This is especially important considering the effects of the dependence of D_L and D_T on the b-value, which introduces two additional coefficients, β_L and β_T.[16,17] It makes such a method more difficult to be used in HP ^{129}Xe experiments: the nearly 3 times lower gyromagnetic
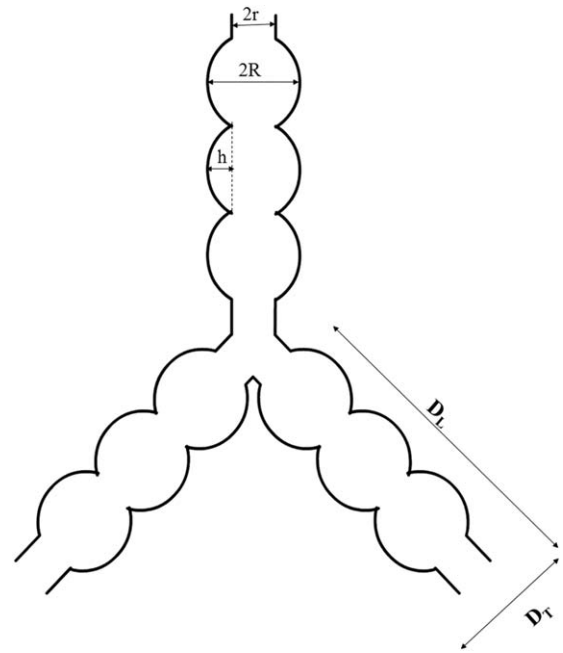

FIGURE 1: Two generations of lung respiratory airways of the Weibel lung model. D_T represents the transverse diffusion coefficient and D_L represents the longitudinal diffusion coefficient. The main morphometric parameters include an external radius (R), an internal radius (r), and a depth of alveolar sleeve (h).

ratio ($\gamma = -11.7$ MHz/T) and the lower spin polarization of ^{129}Xe result in much lower image SNR compared to HP ^{3}He. In addition, the much lower diffusivity of ^{129}Xe requires larger b values to realize sufficient diffusion weighting. This means that stronger gradients and/or longer diffusion time are needed.[16,24] However, these factors accelerate the signal decay of HP ^{129}Xe, leading to further SNR losses. Ouriadov et al. obtained lung morphology with HP ^{129}Xe diffusion MRI and detected the early stage radiation-induced lung injury in a rat model effectively.[20] But the surface area to lung volume ratio (S/V), which is one of the most commonly used to characterize lung morphology (see definitions of these parameters in "An official research policy statement of the ATS" in Ref. 25) was not stated in the study.

The quantification of respiratory airways in vivo is important, and can potentially improve the evaluation of pulmonary diseases at the acinar level, especially the quantification of the S/V. In our study, the morphological parameters of the lung respiratory airways were measured in a rat model to demonstrate the feasibility of quantifying lung respiratory airways in vivo with hyperpolarized xenon diffusion MRI. Accordingly, it was able to detect mild emphysema.

Materials and Methods

Animal Preparation

All animal handling procedures were approved by the institutional Animal Studies Committee. In this study, 10 Sprague Dawley (SD) male rats (233 ± 13 g) were divided into two groups. The study group consisting of five rats was induced to mild emphysema by elastase (Biosharp,
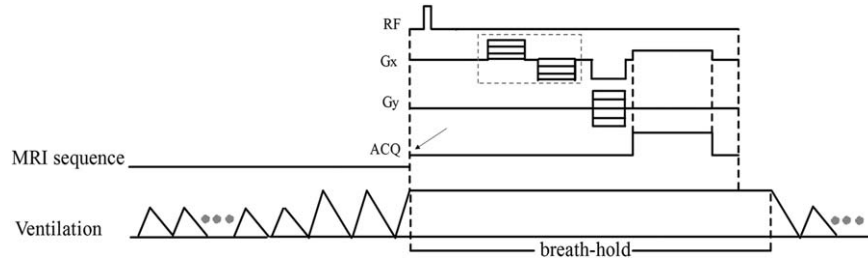
FIGURE 2: The schematic diagram of timing sequence for ventilation and MRI acquisitions. Note the diffusion sensitive gradients as shown in the dashed box during one breath-hold.

Hefei, China) according to a previously developed protocol.[26] To obtain the mild emphysematous rats, experiments were performed 4 weeks post-instillation to allow alveolar breaking by the instillation of elastase. The remaining five rats served as the control group.

Prior to the MRI, each rat was anesthetized with 5.0% of isoflurane (Keyuan Pharmaceutical, Shandong, China), intubated with a 14G endotracheal tube, which was tied to the trachea. After the intubation the rat was ventilated by a homebuilt ventilator, which was computer-controlled using a programmed software based on LabVIEW (National Instruments, Austin, TX). The rat was alternately ventilated with O_2 and HP xenon. For the ventilation of O_2, the breath rate was 50 breaths per minute with inspiratory time of 400 msec and expiratory time of 800 msec. The peak inspiratory pressure was 10 cmH_2O, with inspiratory capacity of about 2.2 mL per breath. After 5 minutes the concentration of isoflurane was turned down to 3% for maintenance. For the ventilation of HP xenon, the breath rate was 15 breaths per minute, with inspiratory time of 500 msec, breath-hold time of 2500 msec, and expiratory time of 1000 msec. The peak inspiratory pressure was 12 cmH_2O, with inspiratory capacity of about 2.5 mL per breath.

The MRI acquisitions were triggered synchronously at the beginning of each breath-hold (arrow in Fig. 2) and ended during the breath-hold. Two times flushing with xenon gas was performed to reduce the oxygen left in the lungs as much as possible before the xenon breath-hold. After the MRI acquisitions the rats were ventilated to regularly breathe normal O_2 again.

^{129}Xe Polarization and MRI

Enriched xenon gas (86% ^{129}Xe) was polarized to ~10% using a homebuilt xenon polarizer using the technique of spin-exchange optical pumping. The gas mixture consisted of 2% xenon, 10% N_2, and balanced ^{4}He. First, the gas mixture was introduced into the glass optical cell of the polarizer and then the ^{129}Xe was polarized via a standard optical pumping process.[5,27] A homebuilt device was developed for accumulating the HP xenon. With such a device the resulting HP xenon was then cryogenically stored in a cold trap with liquid nitrogen at 77 K, and 240 mL HP xenon gas could be obtained after 40 minutes with a flow rate of 0.3 L/min. After collection, HP xenon in the cold trap was thawed into gas with hot water and sublimated into a Tedlar bag. Finally, the Tedlar bag containing HP xenon was connected to the ventilator.

All the MRI experiments were performed on a 7T MRI system (Bruker BioSpec 70/20 USR, Billerica, MA) equipped with a high-performance gradient coil (G_{max} = 444.75 mT/m). A homebuilt, 5.5 cm diameter double-tuned birdcage radiofrequency (RF) coil operating at 298.69 MHz (^{1}H) and 83.07 MHz (^{129}Xe) was used.

The diffusion MRI protocol for the study was obtained based on a gradient-echo sequence with the bipolar gradients in the frequency-encoding direction. The corresponding MRI parameters were as follows: field of view (FOV) = 5 × 5 cm; matrix size = 64 × 64; TE/TR = 5.65/11.26 msec; bandwidth = 50 kHz, and flip angle was 9.5°. The parameters of the diffusion gradient pulse were as follows: ramp up/down time = 0.123 msec; constant time δ and diffusion time Δ were $\delta = \Delta = 2$ msec, which are normally selected between 1 msec to 3 msec for rats.[16] There were eight b values (b = 5, 10, 15, 20, 25, 30, 35, 40 s/cm^2) with the max diffusion gradient 123 mT/m. The 1-msec block excitation RF pulse was used and the excitation bandwidth was 1280 Hz, which ensured a minimal excitation bandwidth to cover the signals of ^{129}Xe dissolved in lung tissue and blood.

Most notably, no observable recovery of longitudinal magnetization takes place after RF pulses, and during HP ^{129}Xe MRI there always exists uncontrollable processes such as T_1 relaxation and dissolution of xenon gas into tissue and blood of lungs. All these factors lead to a steadily declining magnitude of the magnetization, which would affect the results of HP ^{129}Xe diffusion MRI, especially with multi-b values. To reduce these influences, three interleaved 2D gradient-echo sampling were acquired for each line of k-space. Three images were acquired per b value during one breath-hold to ensure that for every b value there existed two corresponding images without a diffusion gradient, ie, the first and third images without a diffusion gradient, while the second image with a diffusion gradient.

Image Processing and Analysis

The MR data was analyzed in MatLab (MathWorks, Natick, MA). To ensure data accuracy, the original k-space MRI data was used in the following analysis. All images were generated from MRI k-space using 2D discrete Fourier transform (DFT). The two images without diffusion gradient were averaged and used to generate lung binary mask without background noise and main tracheas by image segmentation. The resulting binary mask was applied to the source image with diffusion gradient. Accordingly, we have the anisotropic diffusion equation[18]:

$$S = S_0 \int_0^\pi \alpha * \frac{sin\alpha}{2} exp[-b * (D_L cos^2\alpha + D_T sin^2\alpha)]d\alpha$$

$$(1)$$

$$D_M = \frac{1}{3}D_L + \frac{2}{3}D_T$$

$$D_{AN} = D_L - D_T$$

the D_L and D_T can be extracted by fitting the S/S_0 at eight different b values using a nonlinear least squares algorithm on a pixel-
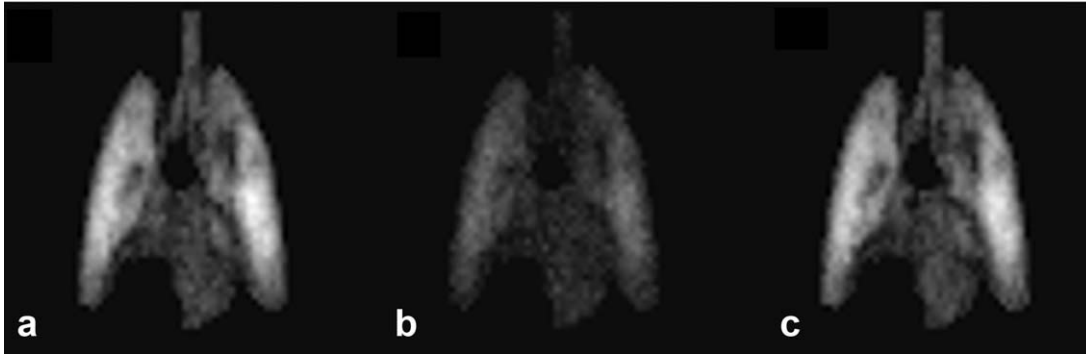
FIGURE 3: Representative three interleaved 2D gradient-echo images in one breath-hold. a: The first image with b = 0 s/cm². b: The second image with b = 40 s/cm² with diffusion gradient field strength 123 mT/m. c: The third image with b = 0 s/cm² again.

by-pixel basis for all the rats. D_M and D_{AN} represent the mean ADC and the anisotropy of ADC, respectively. Yablonskiy et al.[18] proposed a relation between D_T and R based on ^{3}He. Compared to ^{3}He, ^{129}Xe has a very different value for D_0 (the free diffusion coefficient). By replacing the D_0, δ, and Δ, the relationship for D_T and the R based on ^{129}Xe diffusion could be acquired. In addition, the approximate equation existed[18]:

$$D_L = D_0 \left(\frac{r}{R}\right)^2 \qquad (2)$$

if the lung respiratory airways are open. In fact, the xenon atoms reside primarily within the same airway throughout the diffusion gradient pulse, with a diffusion time of 2 msec. In such conditions, it can be assumed that the respiratory airways were "noncommunicating."[23] Here, the pure xenon free diffusion coefficient (0.06 cm²/s) approximates the D_0 in the lungs. Using the calculated lung respiratory airways parameters, some other microgeometric parameters can also been estimated based on the following equations[21]:

$$S_a = \frac{\pi}{4} RL + \frac{\pi}{4} h(2R - h) + 2hL$$
$$V_a = \frac{\pi}{8} R^2 L \qquad (3)$$
$$S/V = S_a/V_a = 4/L_m$$

Histology

After the MRI, the rat was bled to death from a quick cut in two sides of the femoral artery. The whole lung was extracted and filled to an airway pressure of 25 cm H_2O with a 10% paraformaldehyde solution (Sinopharm, Shanghai, China) for 30 minutes. Then it was placed in the same solution for at least 24 hours.[28,29] Finally, the solidified lung was made into hematoxylin and eosin (H&E)-stained histological sections. Six histological sections from different regions were obtained from each lung and each section was 10 μm thick. These histological sections were observed under a microscope (Nikon Eclipse Ts 100) and corresponding images were acquired. Image-Pro Plus software was used to compute the mean linear intercept (Lm) for each image so that each rat would have six Lm values from different sections. To reduce the random error, the Lm values were averaged after the maximum one and the

minimal one were taken out. The mean Lm value was used to represent the Lm of the rat.

Statistical Analysis

A paired t-test was used to assess the significance of changes of the histological Lm in the mild emphysematous group and the control group. The mean anisotropic diffusion parameters (D_L, D_T, D_M, and D_{AN}) and the parameters of respiratory airways in vivo from HP ^{129}Xe diffusion MRI were fitted and calculated in all the rats. A paired t-test was also used to assess the significance of changes about these parameters in the mild emphysematous group and the control group. Meanwhile, Pearson's correlation coefficients were calculated for the parameters between HP ^{129}Xe diffusion MRI and the histological Lm. In addition, a Bland–Altman graph was used to evaluate the consistency of the Lm obtained by the two different methods. The results were used to evaluate the rationality and accuracy of the method in vivo to detect mild emphysema. $P < 0.05$ was considered statistically significant.

Results

Figure 3 shows three representative interleaved 2D lung gradient-echo images acquired during a single breath-hold. Figure 3a,c were acquired with $b = 0$ s/cm², whereas Fig. 3b with $b = 40$ s/cm². Due to the diffusion of xenon atoms in the lung, Fig. 3b was much darker than Fig. 3a,c. We note that the image quality remained good in spite of the long echo time and the lack of any filtering applied.

Figure 4 shows a typical plot to fit the S/S_0 at eight different b values using a nonlinear least squares algorithm. The signal intensities were taken from the regions of interest, as shown in the red box of the inset. The fitting was very good (R-Square = 0.98).

Table 1 lists the mean values of overall parameters including the Lm obtained from histology, the ^{129}Xe anisotropic diffusion coefficients (D_L, D_T, D_M, D_{AN}), and the measured results of the lung respiratory airways (R, r, h, Lm, S/V) in the emphysematous and the control groups. The Lm from histology showed a significant increase in the emphysematous group compared to that in the control group ($P = 0.005$). The mean Lm was 101.42 μm in the emphysematous rats and 81.52 μm in the healthy rats.
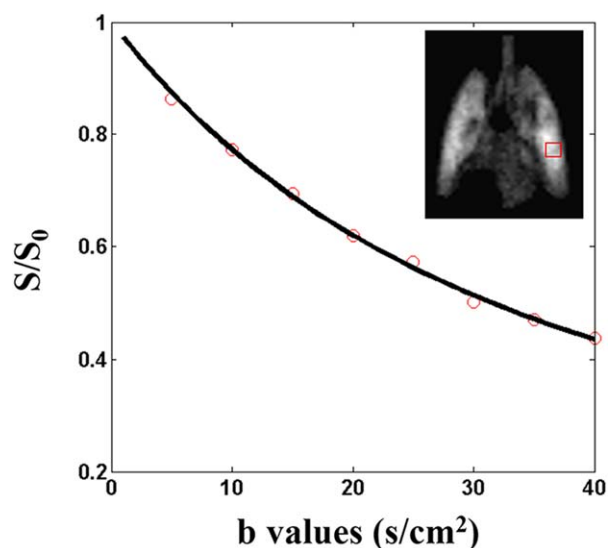
FIGURE 4: Using signal intensities in a region of interest (box), shown in the inset. A typical fitting of the S/S_0 vs b values was plotted. The R-Square was 0.98.

Figure 5 displays two representative H&E-stained lung histological sections from the emphysematous rat E_1 (Fig. 5a) and the healthy rat H_1 (Fig. 5b), which intuitively reflected the destruction, mainly the enlargement of pulmonary airspace, in the emphysematous rat.

The mean values of all ^{129}Xe anisotropic diffusion coefficients (D_L, D_T, D_M, D_{AN}) were larger in the emphysematous group in comparison to those in the control group. Especially D_L, D_M, and D_{AN} showed a significant increase ($P < 0.05$). The results obtained by HP ^{129}Xe diffusion MRI were consistent with those observed in the histological sections. Moreover, the correlations between the D_L, D_M, and D_{AN} to the Lm were very good for all the rats ($r > 0.8$). However, D_T exhibited no significant difference ($P = 0.084$) between the emphysematous group and the control group, and the Pearson's correlation coefficient was only 0.68. Figure 6 presents the representative ^{129}Xe anisotropic diffusion coefficient (D_L, D_T, D_M, and D_{AN}, from left to right) maps for the emphysematous rat E_1 (line a) and the healthy rat H_1 (line b).

The Lm represents the mean linear intercept from HP ^{129}Xe diffusion MRI, and the values exceeding 200 μm were considered unreasonable and treated as outliers. Surprisingly, all the mean Lm values obtained by HP ^{129}Xe diffusion MRI were larger systematically than those obtained from histological sections. The systematic differentials were about 30 μm. However, note the elevated mean R, r, and Lm and the depressed mean h and S/V in the emphysema rats, and the difference was significant ($P < 0.05$), except R ($P = 0.089$). Meanwhile, these parameters of the lung respiratory airways in all the rats correlated highly with the Lm from histology ($r > 0.8$), except the R ($r = 0.68$). Figure 6 also presents the representative maps of lung respiratory

airways parameters R, r, h, and S/V in the corresponding emphysematous rat E_1 (line c) and the healthy rat H_1 (line d). Note the changes of the r and S/V maps in the emphysematous rat.

Figure 7 shows a Bland–Altman graph to evaluate the consistency of the two methods to measure Lm. The methods were HP ^{129}Xe diffusion MRI and the histological sections, respectively. All the dots were within the two 95% consistency limit lines, which indicated that it was feasible to measure Lm with HP ^{129}Xe diffusion MRI. However, note the position of the dashed line, which reflected that a systematic differential existed.

Figure 8 shows the correlations of the representative parameters including D_L, r, h, and S/V obtained by HP ^{129}Xe diffusion MRI to Lm from histology, the reference standard to evaluate the pulmonary morphology for all the rats. Solid lines represent linear regression and dashed lines represent 95% confidence intervals for these fits. Note that all the dots were within the dashed lines, which indicated that the correlations between the parameters obtained by HP ^{129}Xe diffusion MRI and the Lm from histology were good and credible. The corresponding Pearson's correlation coefficients can be found in Table 1.

Discussion

In this study, HP ^{129}Xe diffusion MRI with eight b values was used to measure and quantify the lung respiratory airways of 10 rats based on the Weibel lung model, and the acquired parameters were used to detect the mild emphysematous rats for the first time. Although the effect of the dependence of D_L and D_T on b-value was not taken into account, the D_L, r, h, Lm, and S/V obtained by HP ^{129}Xe diffusion MRI exhibited significant differences in the mild emphysematous rats compared to those in the control rats. These parameters correlated strongly with the Lm derived from histology, the reference standard to evaluate pulmonary morphology. The lung morphological measurement in rats with HP xenon in vivo was previously reported by Ouriadov et al.[20] The corresponding parameters of morphology in the healthy rats could be compared. The mean h of 36 μm in the healthy rats in our study was very similar to the value of 33 μm in Ouriadov's study.[20] But the mean external airway radius R of 128 μm and r of 92 μm were a little larger than that R of 100 μm and r of 67 μm in their studies.[20] Richard et al. studied the pulmonary air spaces in rats with 3D MRI of non-Gaussian ^{3}He gas diffusion and their acquired median value of R was 160 μm, but they did not compute the average value of R.[15] Meanwhile, the mean R value for healthy mice obtained with ^{3}He studies was in the range of 97–105 μm,[30,31] and it is reasonable that the R = 128 μm of rats was larger than that of mice. The S/V is one of the most commonly used parameters to characterize lung morphology and evaluate emphysema.[10,30] In comparison to the

TABLE 1. Overall List of the Lm From Histology and the Corresponding Obtained Parameters With HP ^{129}Xe Diffusion MRI in the Lung of the Emphysematous Rats (n = 5) and the Healthy Rats (n = 5)

		Lm(μm) (histology)	$D_{L\times10}^{-2}$ (cm^2/s)	$D_{T\times10}^{-2}$ (cm^2/s)	$D_{M\times10}^{-2}$ (cm^2/s)	$D_{AN\times10}^{-2}$ (cm^2/s)	R(μm)	r(μm)	h(μm)	Lm(μm)	S/V(cm^{-1})
Emphysematous rats	E_1	102.82 ± 12.10	5.29 ± 0.07	1.39 ± 0.03	2.69 ± 0.03	3.90 ± 0.11	136.41 ± 2.13	108.44 ± 1.65	27.97 ± 0.48	125.18 ± 0.29	259.61 ± 3.17
	E_2	106.62 ± 11.87	5.72 ± 0.46	1.35 ± 0.05	2.81 ± 0.12	4.36 ± 0.51	134.24 ± 4.03	112.13 ± 0.43	22.12 ± 4.46	142.33 ± 1.52	228.39 ± 18.91
	E_3	102.76 ± 4.16	4.92 ± 0.18	1.31 ± 0.06	2.51 ± 0.06	3.61 ± 0.18	131.08 ± 0.37	100.59 ± 1.40	30.49 ± 1.03	120.09 ± 0.36	284.15 ± 1.15
	E_4	97.25 ± 5.77	5.37 ± 0.26	1.33 ± 0.05	2.68 ± 0.05	4.05 ± 0.31	132.85 ± 4.12	106.18 ± 1.04	26.67 ± 3.08	129.32 ± 9.07	254.66 ± 22.95
	E_5	97.65 ± 9.11	4.83 ± 0.05	1.41 ± 0.10	2.55 ± 0.09	3.43 ± 0.05	136.86 ± 5.83	102.90 ± 5.31	33.96 ± 0.53	120.52 ± 3.78	300.56 ± 16.33
	Mean	**101.42 ± 3.95**	**5.23 ± 036**	**1.36 ± 0.04**	**2.65 ± 0.12**	**3.87 ± 0.37**	**134.29 ± 2.42**	**106.04 ± 4.54**	**28.24 ± 4.41**	**127.49 ± 9.12**	**265.47 ± 27.87**
Healthy rats	H_1	76.95 ± 4.56	3.29 ± 0.78	1.18 ± 0.08	1.89 ± 0.21	2.11 ± 0.85	124.49 ± 4.57	81.23 ± 1.29	43.25 ± 5.87	100.52 ± 6.14	377.87 ± 37.20
	H_2	80.30 ± 1.84	4.34 ± 0.32	1.24 ± 0.07	2.27 ± 0.06	3.10 ± 0.39	125.44 ± 0.45	89.64 ± 2.25	35.80 ± 2.70	115.39 ± 2.38	320.17 ± 10.90
	H_3	78.04 ± 3.79	4.29 ± 0.24	1.16 ± 0.04	2.20 ± 0.05	3.13 ± 0.28	123.84 ± 2.71	88.12 ± 0.11	35.72 ± 2.81	110.89 ± 0.08	322.65 ± 7.39
	H_4	93.48 ± 1.82	5.13 ± 0.37	1.36 ± 0.05	2.62 ± 0.09	3.77 ± 0.42	135.01 ± 2.09	105.06 ± 0.69	29.95 ± 2.78	118.67 ± 1.58	288.76 ± 10.59
	H_5	78.85 ± 4.19	4.52 ± 0.03	1.37 ± 0.07	2.42 ± 0.04	3.14 ± 0.10	135.35 ± 4.49	100.00 ± 3.42	35.34 ± 1.07	116.81 ± 0.75	300.83 ± 8.15
	Mean	**81.52 ± 6.79**	**4.31 ± 0.66**	**1.26 ± 0.10**	**2.28 ± 0.27**	**3.05 ± 059**	**128.82 ± 9.59**	**92.81 ± 9.59**	**36.01 ± 4.74**	**112.46 ± 7.26**	**322.05 ± 34.20**
P-value[a]		0.0005	0.0262	0.0837	0.024	0.0304	0.0890	0.02360	0.0277	0.0204	0.0209
Pearson's correlation coefficient[b]		0.85	0.68	0.68	0.86	0.84	0.68	0.86	-0.85	0.81	-0.83

[a]*P*-values were obtained by a paired *t*-test to quantify the difference between the emphysematous rats and the healthy rats.

[b]Pearson's correlation coefficients were to test correlations of the corresponding parameters obtained by HP ^{129}Xe diffusion MRI to the Lm from histology, the gold standard of evaluating emphysema.
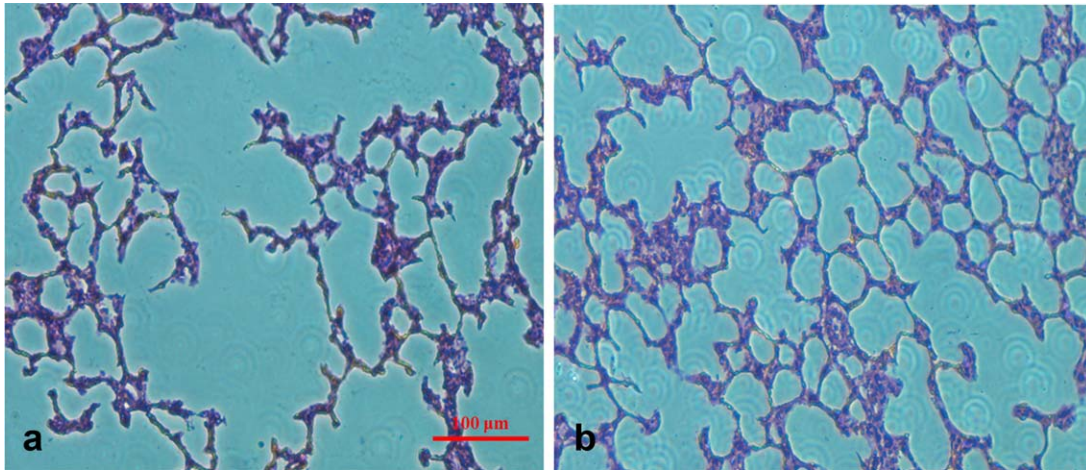
FIGURE 5: Representative images of H&E-stained lung histological sections under the microscope (Nikon Eclipse Ts 100). The magnification was 200. a: A representative emphysematous rat E_1. b: A representative healthy rat H_1. The Lm of these two images was 118.83 μm for image a and 79.20 μm for image b. Note the enlarged airspaces in the emphysematous rat.

S/V values in mice of 698 cm^{-1},[30] and in humans of 200 cm^{-1},[11] it was reasonable that the S/V value in the rats from our experiment fell in between. The results suggested that the lung respiratory airways can be quantified with hyperpolarized xenon diffusion MRI. It can also be used for the detection of mile emphysema.

In comparison to helium, xenon can dissolve in the pulmonary capillary bloodstream,[27,32] which reduces the gas signal and affects the HP ^{129}Xe diffusion MRI, especially the multi-b diffusion MRI. In this study, HP xenon gas of 2.5 mL (STP) in the lung per breath-hold, its solubility of $\sim$14% in the blood, combined with a cardiac output of 0.45 mL/s, reduces the gas concentration in the lung by

6.3% during the 2500 msec breath-hold. If the images for the eight b values are sampled in one breath, the influence will increase significantly. So it is necessary to sample an image with $b = 0$ for every nonzero b value, which would reduce the influence caused by the difference of different b values beyond the different diffusion gradient strengths, such as xenon dissolution, T_1 relaxation, RF depolarization, etc.

The ^{129}Xe D_T values in lungs of the emphysematous group showed no significant difference compared to that of the control group. Considering the time for making the emphysematous rat model and the calculated Lm (101 μm), the emphysema can be classified as of mild intensity.[19] It
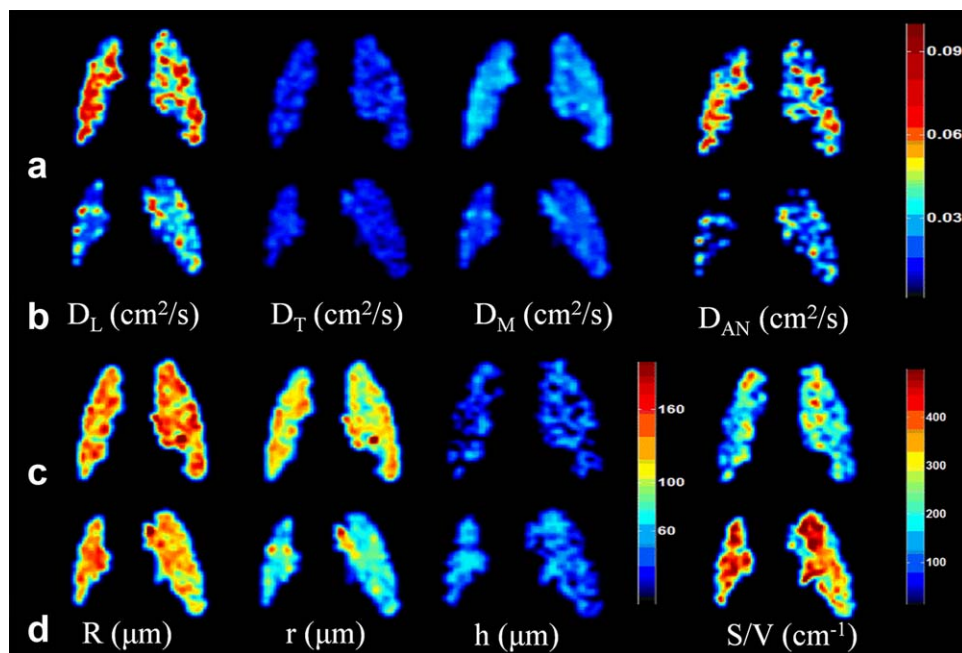

FIGURE 6: Representative maps of xenon anisotropic diffusion coefficients (D_L, D_T, D_M, D_{AN}, from left to right) and parameters of lung respiratory airway R, r, h, and S/V in the corresponding emphysematous rat E_1 (Lines a and c) and the healthy rat H_1 (Lines b and d).
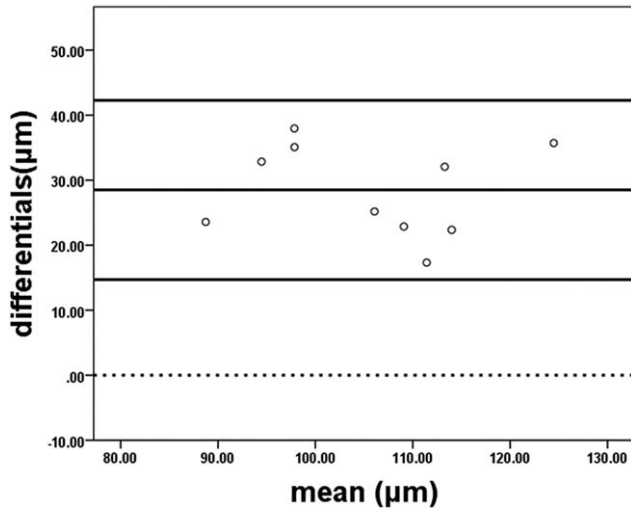
FIGURE 7: Bland–Altman graph to evaluate the consistency of the two methods of measuring the Lm for all the rats. The methods were HP ^{129}Xe diffusion MRI and histological sections, respectively.

was likely that the D_L was more sensitive in the mild emphysema and D_T was more sensitive in the severe emphysema. The same conclusion was also drawn in the previous study of ^{3}He diffusion MRI.[18,33] In those studies, it was speculated that in mild emphysema the change of lung structure was mainly due to expansion of the respiratory airways and collapse of alveolus, but without substantial lung

tissue destruction and pulmonary acinar deformation. This was consistent with the result of lung respiratory airways obtained by HP ^{129}Xe diffusion MRI in this study. The increase of r represented expansion of respiratory airways and the decrease of h represented collapse of alveolus. A similar conclusion was also reported by Fichele et al, who used the finite-difference method to simulate diffusion in 3D alveolar ducts.[34]

The mean Lm value obtained by HP ^{129}Xe diffusion MRI was systematically different for all the rats compared to that from histology. The systematic differentials were about 30 μm. It may be induced by the lung model, which assumes a specific, geometric airway structure, whereas the true lung structure is more complicated. So better models, which are more similar to lungs in vivo, remain to be developed and studied. Another potentially systematic difference depends on the level of lung inflation between the lungs in vivo and the excised lungs. Although the extracted lungs were filled to an airway pressure of 25 cm H_2O with a 10% paraformaldehyde solution to approach the lung status in vivo, it was difficult to keep the lungs in an identical condition as in vivo. The same problem was also encountered in a previous study on mice with HP ^{3}He diffusion MRI.[26]

Considering the low signal of HP ^{129}Xe, there were two simplifications in the qualification of lung respiratory airways with HP ^{129}Xe diffusion MRI. On the one hand,
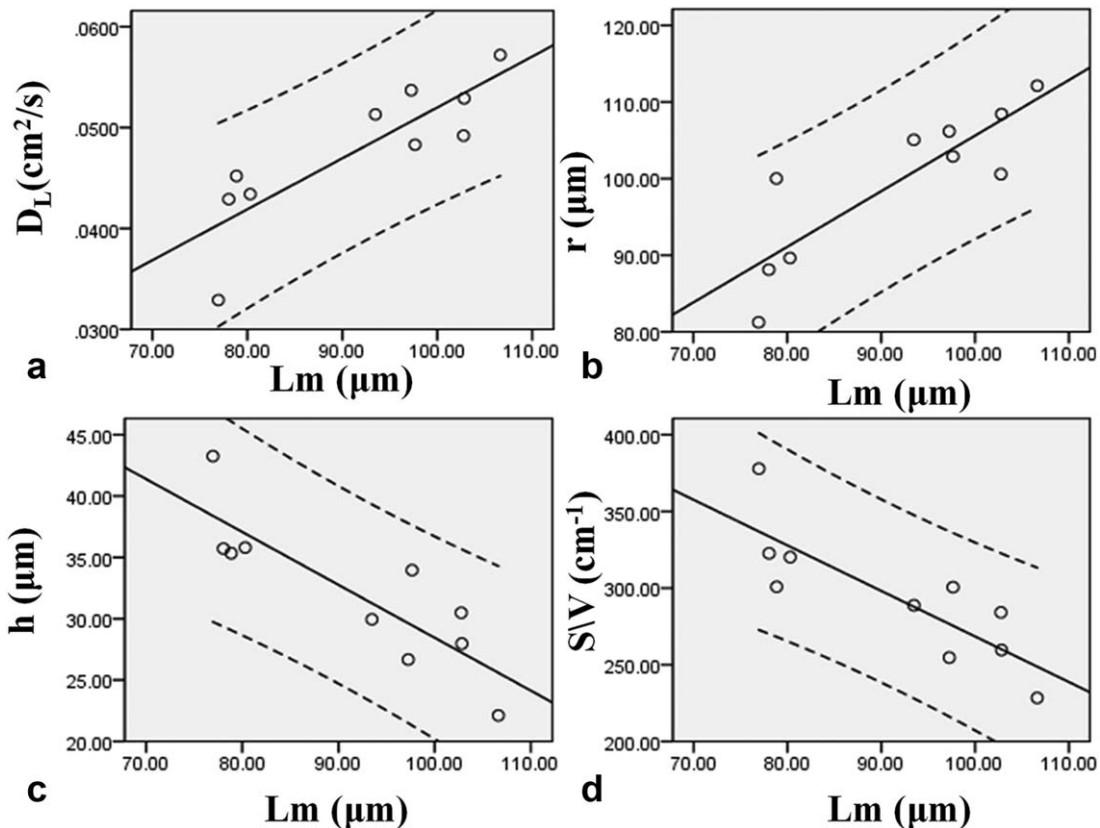

FIGURE 8: The linear correlation fittings with representative parameters obtained in vivo by HP xenon diffusion MRI vs. Lm from histology. Solid lines represent linear regression line and dashed lines represent 95% confidence intervals for these fits.

the effects of dependence of D_L and D_T on the b-value were not taken into account to reduce the complexity of fitting in this study. According to Yablonskiy et al, the effects would be stronger when the max b value is higher. In our study, the max b value was 40 cm^2/s, which was much smaller than the previous study in rats of radiation-induced lung injury[20] and the dependence of D_L and D_T on b values would be much smaller. In fact, due to the limitation of gradient strength in clinical studies and the low SNR for HP ^{129}Xe images, the max b values are much more limited in human studies. On the other hand, D_0 in lungs was $\sim$0.06 cm^2/s, which was the pure xenon free diffusion coefficient. In fact, the diffusion coefficient D_0 depends on gas concentration in lung airspaces. Although two times flushing of xenon was applied before the breath-hold, the concentration of xenon in the lungs could not reach 100% and the actual D_0 value of xenon in lungs should be bigger than 0.06 cm^2/s.

There were still some limitations in the experiment. To improve image SNR, the images of eight b values were acquired in separate breath-holds in our study. Although the breathing xenon volume was the same every time for the rats, the pulmonary status for every breath-hold was hardly kept completely identical. Slight pulmonary status differences existed when images with different b values were acquired. In addition, although the histological sections could reflect the pulmonary microstructure directly, they were from partial regions of the lungs and hardly displayed the global state of the lung structure. In the future, high-resolution animal CT may be used to obtain the 3D images of the global lungs, which will be more accurate for comparison with results of HP xenon diffusion MRI. Although multi-b HP ^{129}Xe diffusion MRI in this study provided a valid method to detect the mildly emphysematous rats and quantify the microstructure of lung respiratory airways, it was still hard to locate the lung lesions due to the limited SNR and resolution images. It is necessary to improve the xenon polarizers and obtain higher xenon polarization.[35] Meanwhile, the closely coupled multichannel receive arrays[36] and parallel imaging techniques[37,38] should also be adopted to acquire higher image SNR and resolution. Further, the newly presented HP gas MRI methods can also be combined.[39,40] This will make it possible to detect the parenchymal local lesions. The method of quantification for lung respiratory airways will provide local microstructural information in alveoli, which will be very useful for clinical early pulmonary disease diagnosis and therapy, especially the early emphysema or COPD.

In conclusion, the restricted Brandon motion of HP gas in the lungs is closely related to the surrounding condition, so HP ^{129}Xe diffusion MRI is very sensitive to the change of pulmonary parenchymal microstructure. The study demonstrated the feasibility of HP xenon diffusion MRI to quantify the pulmonary respiratory airways. It could be used to detect emphysematous lungs in rats. Meanwhile, the results also suggested that the D_L of HP ^{129}Xe in the lungs is more sensitive than D_T to detect mild emphysema. It opens a door for diagnosis of lung diseases, noninvasively, especially for emphysema.

References

1. Chen XJ, Hedlund LW, Möller HE, Chawla MS, Maronpot RR, Johnson GA. Detection of emphysema in rat lungs by using magnetic resonance measurements of ^{3}He diffusion. Proc Natl Acad Sci U S A 2000; 97:11478–11481.

2. Rabe KF, Hurd S, Anzueto A, et al. Global strategy for the diagnosis, management, and prevention of chronic obstructive pulmonary disease — GOLD executive summary. Am J Respir Crit Care Med 2007; 176:532–555.

3. Gevenois PA, Yernault JC. Can computed tomography quantify pulmonary emphysema? Eur Respir J 1995;8:843–848.

4. Zhou X. Hyperpolarized noble gases as contrast agents. In: Schröder L, Faber C, editors. In vivo NMR imaging. New York: Humana Press; 2011. p 189–204.

5. Mugler JP, Altes TA. Hyperpolarized ^{129}Xe MRI of the human lung. J Magn Reson Imaging 2013;37:313–331.

6. Capozzi A, Roussel C, Comment A, Hyacinthe JN. Optimal glass-forming solvent brings sublimation dynamic nuclear polarization to Xe-129 hyperpolarization biomedical imaging standards. J Phys Chem C 2015;119:5020–5025.

7. Svenningsen S, Kirby M, Starr D, et al. Hyperpolarized ^{3}He and ^{129}Xe MRI: differences in asthma before bronchodilation. J Magn Reson Imaging 2013;38:1521–1530.

8. Wang CB, Mugler JP, de Lange EE, Patrie JT, Mata JF, Altes TA. Lung injury induced by secondhand smoke exposure detected with hyperpolarized helium-3 diffusion MR. J Magn Reson Imaging 2014; 39:77–84.

9. Diaz S, Casselbrant I, Piitulainen E, et al. Hyperpolarized ^{3}He apparent diffusion coefficient MRI of the lung: reproducibility and volume dependency in healthy volunteers and patients with emphysema. J Magn Reson Imaging 2008;27:763–770.

10. Yablonskiy DA, Sukstanskii AL, Quirk JD, Woods JC, Conradi MS. Probing lung microstructure with hyperpolarized noble gas diffusion MRI: theoretical models and experimental results. Magn Reson Med 2014;71:486–505.

11. Woods JC, Choong CK, Yablonskiy DA, et al. Hyperpolarized ^{3}He diffusion MRI and histology in pulmonary emphysema. Magn Reson Med 2006;56:1293–1300.

12. Salerno M, de Lange EE, Altes TA, Truwit JD, Brookeman JR, Mugler JP. Emphysema: Hyperpolarized helium-3 diffusion MR imaging of the lungs compared with spirometric indexes — initial experience. Radiology 2002;222:252–260.

13. Mugler JP, Mata JF, Wang HTJ, et al. The apparent diffusion coefficient of [129]Xe in the lung: preliminary results. In: Proc 12th Annual Meeting ISMRM, Kyoto; 2004 (abstract 769).

14. Mata JF, Altes TA, Cai J, et al. Evaluation of emphysema severity and progression in a rabbit model: comparison of hyperpolarized [3]He and [129]Xe diffusion MRI with lung morphometry. J Appl Physiol 2007;102:1273–1280.

15. Jacob RE, Laicher G, Minard KR. 3D MRI of non-Gaussian [3]He gas diffusion in the rat lung. J Magn Reson 2007;188:357–366.

16. Sukstanskii AL, Yablonskiy DA. Lung morphometry with hyperpolarized [129]Xe: theoretical background. Magn Reson Med 2012;67:856–866.

17. Sukstanskii AL, Yablonskiy DA. In vivo lung morphometry with hyperpolarized [3]Hediffusion MRI: theoretical background. J Magn Reson 2008;190:200–210.

18. Yablonskiy DA, Sukstanskii AL, Leawoods JC, et al. Quantitative in vivo assessment of lung microstructure at the alveolar level with hyperpolarized [3]He diffusion MRI. Proc Natl Acad Sci U S A 2002;99:3111–3116.

19. Tanoli TSK, Woods JC, Conradi MS, et al. In vivo lung morphometry with hyperpolarized [3]He diffusion MRI in canines with induced emphysema: disease progression and comparison with computed tomography. J Appl Physiol 2007;102:477–484.

20. Ouriadov A, Fox M, Hegarty E, Parraga G, Wong E, Santyr GE. Early stage radiation-induced lung injury detected using hyperpolarized [129]Xe Morphometry: proof-of-concept demonstration in a rat model. Magn Reson Med 2016;75:2421–2431.

21. Yablonskiy DA, Sukstanskii AL, Woods JC, et al. Quantification of lung microstructure with hyperpolarized [3]He diffusion MRI. J Appl Physiol 2009;107:1258–1265.

22. Quirk JD, Sukstanskii AL, Woods JC, et al. Experimental evidence of age-related adaptive changes in human acinar airways. J Appl Physiol 2016;120:159–165.

23. Sukstanskii AL, Conradi MS, Yablonskiy DA. [3]He lung morphometry technique: accuracy analysis and pulse sequence optimization. J Magn Reson 2010;207:234–241.

24. Ouriadov A, Farag A, Kirby M, McCormack DG, Parraga G, Santyr GE. Lung morphometry using hyperpolarized [129]Xe apparent diffusion coefficient anisotropy in chronic obstructive pulmonary disease. Magn Reson Med 2013;70:1699–1706.

25. Hsia CC, Hyde DM, Ochs M, Weibel ER. An official research policy statement of the American Thoracic Society/European Respiratory Society: standards for quantitative assessment of lung structure. Am J Respir Crit Care Med 2010;181:394–418.

26. Chino K, Choong CK, Toeniskoetter PD, et al. A canine model for production of severe unilateral panacinar emphysema. Exp Lung Res 2004;30:319–332.

27. Li H, Zhang Z, Zhao X, Sun X, Ye C, Zhou X. Quantitative evaluation of radiation-induced lung injury with hyperpolarized xenon magnetic resonance. Magn Reson Med 2016;76:408–416.

28. Boudreau M, Xu X, Santyr GE. Measurement of [129]Xe gas apparent diffusion coefficient anisotropy in an elastase-instilled rat model of emphysema. Magn Reson Med 2013;69:211–220.

29. Blumler P, Acosta RH, Thomas-Semm A, Reuss S. Lung fixation for the preservation of air spaces. Exp Lung Res 2004;30:73–82.

30. Wang W, Nguyen NM, Yablonskiy DA, et al. Imaging lung microstructure in mice with hyperpolarized [3]He diffusion MRI. Magn Reson Med 2011;65:620–626.

31. Osmanagic E, Sukstanskii AL, Quirk JD, et al. Quantitative assessment of lung microstructure in healthy mice using an MR-based [3]He lung morphometry technique. J Appl Physiol 2010;109: 1592–1599.

32. Qing K, Ruppert K, Jiang Y, et al. Regional mapping of gas uptake by blood and tissue in the human lung using hyperpolarized xenon-129 MRI. J Magn Reson Imaging 2014;39:346–359.

33. Gierada DS, Woods JC, Bierhals AJ, et al. Effects of diffusion time on short-range hyperpolarized [3]He diffusivity measurements in emphysema. J Magn Reson Imaging 2009;30:801–808.

34. Fichele S, Paley MN, Woodhouse N, Griffiths PD, Van Beek EJ, Wild JM. Finite-difference simulations of [3]He diffusion in 3D alveolar ducts: comparison with the "cylinder model." Magn Reson Med 2004;52: 917–920.

35. Zhou X, Graziani D, Pines A. Hyperpolarized xenon NMR and MRI signal amplification by gas extraction. Proc Natl Acad Sci U S A 2009; 106:16903–16906.

36. Lee RF, Johnson G, Stefanescu C, Trampel R, McGuinness G, Stoeckel B. A 24-ch phased-array system for hyperpolarized helium gas parallel MRI to evaluate lung functions. In: Proc IEEE-EMBS 27th Annual International Conference, Shanghai, China; 2005. p 4278.

37. Chang YV, Quirk JD, Yablonskiy DA. In vivo lung morphometry with accelerated hyperpolarized [3]He diffusion MRI: a preliminary study. Magn Reson Med 2015;73:1609–1614.

38. Salerno M, Altes TA, Brookeman JR, de Lange EE, Mugler JP. Rapid hyperpolarized [3]He diffusion MRI of healthy and emphysematous human lungs using an optimized interleaved-spiral pulse sequence. J Magn Reson Imaging 2003;17:581–588.

39. Deng H, Zhong J, Ruan W, et al. Constant-variable flip angles for hyperpolarized media MRI. J Magn Reson 2016;263:2–100.

40. Collier GJ, Wild JM. In vivo measurement of gas flow in human airways with hyperpolarized gas MRI and compressed sensing. Magn Reson Med 2015;73:2255–2261.